Synthesis of oxomolybdenum bis(dithiolene) complexes related to the cofactor of the oxomolybdoenzymes†

E. Stephen Davies, Roy L. Beddoes, David Collison, Andrew Dinsmore, Arefa Docrat, John A. Joule, Clare R. Wilson and C. David Garner*

Chemistry Department, The University of Manchester, Oxford Road, Manchester, UK M13 9PL

A synthetic strategy is reported for a general route to asymmetric dithiolenes. This has been used for the generation of $[MoO(dithiolene)_2]^{2-}$ complexes [dithiolene = $^-SC(H)C(R)S^-$, R = phenyl, pyridin-2-yl, pyridin-3-yl, pyridin-4-yl, quinoxalin-2-yl or 2-(dimethylaminomethyleneamino)-3-methyl-4-oxopteridin-6-yl], which have been characterised by analysis, spectroscopy and electrochemistry. The prototypical compound $[PPh_4]_2[MoO(sdt)_2]\cdot EtOH$, where sdt = α,β-styrenedithiolate (R = phenyl), crystallises in the space group $P2_1/c$ with $a = 13.217(4)$, $b = 31.820(8)$, $c = 14.534(7)$ Å, $\beta = 113.8(2)°$ and $Z = 4$. The $MoOS_4$ moiety is square-based pyramidal with the O atom at the apex [Mo=O, 1.700(5) Å] and contains a *cis* geometry of the phenyl groups. The physical properties of all the compounds are consistent with a retention of the $MoOS_4$ centre and the variation in the dithiolene ^1H NMR resonances, infrared ν(Mo=O) and ν(C=C) stretching frequencies and the $E_{\frac{1}{2}}$ values for the Mo^V–Mo^{IV} couple are rationalised by a consideration of the nature of the R substituent. The complexes with the pterin [2-amino-4(1*H*)-pteridinone] substituent have a particular relevance to the Mo centre in oxomolybdoenzymes, and are the closest structural models to date for these enzymes containing two molybdopterin ligands per metal.

The concept that a small molybdenum-containing unit might act as a cofactor for the molybdoenzymes was first suggested by Pateman *et al.*[1] over 30 years ago; as a result of work on a series of mutant cells lacking both nitrate reductase and xanthine oxidase activity, it was proposed that the two enzymes share a common cofactor. Support for this idea came from work by Nason and co-workers[2] and, based on the reconstitution of a molybdenum-deficient nitrate reductase from a mutant strain of *Neurospora crassa*, Nit-1, the concept of a molybdenum cofactor, Moco, common to molybdoenzymes was developed.[3–7] Thus, activity has been returned to Nit-1 nitrate reductase using cofactor produced from other oxomolybdoenzymes, *e.g.* aldehyde oxidase, sulfite oxidase and nitrate reductase. Molybdenum cofactor, or minor structural variants thereof, is also the cofactor for xanthine oxidase, pyridoxal oxidase, nicotinate oxidase, carbon monoxide oxidase, formate dehydrogenase, tetrathionate reductase, chlorate reductase, biotin sulfoxide reductase, purine hydroxylase and dimethyl sulfoxide reductase (DMSOR), enzymes all involved in overall two-electron/oxygen atom transfer processes.

The first steps in the elucidation of the nature of Moco were achieved by Rajagopalan and co-workers[8,9] who showed that an essential component was a pterin [2-amino-4(1*H*)-pteridinone] with a unique functionality containing two sulfur atoms which are bound to Mo. A variety of degradative chemical studies and spectroscopic investigations led Rajagopalan and co-workers to propose a structure for Moco which, in virtually all of its essential details, has been confirmed by protein crystallographic studies of the oxomolybdoenzymes.

The basis for understanding the chemistry of the oxomolybdoenzymes has advanced enormously as a result of these crystallographic determinations for enzymes of this class.[10–14] The first report of the structure of a 'molybdopterin' (mpt)-containing enzyme (see Fig. 1) was achieved for the tungsten aldehyde ferredoxin oxidoreductase from *Pyrococcus furiosus.*[15] 'Molybdopterin' is a reduced pterin, carrying a pyran ring with a dithiolene function which serves as a bidentate ligand for Mo and W in these enzymes; in some enzymes the phosphate group is linked to a nucleotide. The protein crystallographic results showed for the first time that some oxomolybdoenzymes, *e.g.* aldehyde oxidoreductase,[10] have one mpt attached to the metal whilst others, DMSO reductase[11–13] and formate dehydrogenase H,[14] have two mpt's per Mo.

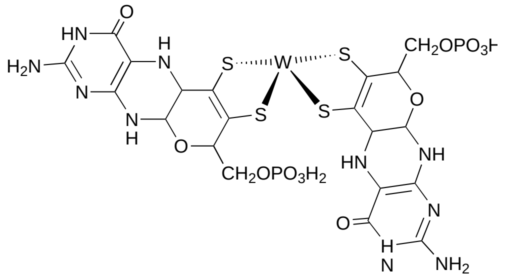

Fig. 1 Diagrammatic representation of the tungsten cofactor of aldehyde ferredoxin oxidoreductase,[15] which does not show the mpt's bridged by Mg^{2+} through the two phosphate groups. Tungsten-oxo group(s) identified by EXAFS measurements were not located in the crystallographic determination

The protein crystallographic results show that Moco contains some structural facets which are not reproduced by simple, low molecular weight co-ordination complexes previously regarded as good analogues of the Mo centres of the enzymes. Given that it has not yet been possible to isolate Moco as released from its associated protein, we have embarked upon the synthesis of this entity. This paper reports the development of our synthetic strategy to date and indicates the spectroscopic and electrochemical properties of the resultant molybdenum complexes.

Experimental

Materials

Quinoxaline, 2-, 3- and 4-acetylpyridine and phenacyl bromide were obtained from Lancaster Synthesis Ltd. The salt $K_4[MoO_2(CN)_4]\cdot 6H_2O$,[16,17] 2-(*N*,*N*-dimethylamino)-4-(R)-1,3-

---

† Based on the presentation given at Dalton Discussion No. 2, 2nd–5th September 1997, University of East Anglia, UK.

Non-SI unit employed: G = 10^{-4} T.

dithiolium hydrogensulfate (R = pyridin-3-yl or quinoxalin-2-yl)[18] and 4-(2-*N*,*N*-dimethylaminomethyleneamino)-3-methyl-4-oxopteridin-6-yl-1,3-dithiol-2-one[19] were prepared by literature methods. 2-(*N*,*N*-Dimethylamino)-4-(pyridin-4-yl)-1,3-dithiolium hydrogensulfate was synthesised by application of the method of Rowe *et al.*[18] The proligands (R)-1,3-dithiol-2-one (R = phenyl, pyridin-2-yl, pyridin-3-yl, pyridin-4-yl or quinoxalin-2-yl) were synthesised by application of the method of Bhattacharya and Hortmann[20] from the corresponding α-bromoketone.

All reactions were performed under an atmosphere of dinitrogen or argon, using standard Schlenk-line techniques. Solvents were either degassed or purged with dinitrogen or argon prior to use.

Microanalyses were conducted by the staff of the Microanalytical Service of the Department of Chemistry, The University of Manchester.

Infrared spectra were collected on either a Perkin-Elmer 1710 Series Fourier-transform IR spectrometer or an ATI Mattson Genesis Series Fourier-transform IR spectrometer. Proton NMR spectra were recorded on either a Bruker AC300E, a Varian Unity Inova 300, a Varian Unity Inova 400 or a Varian Unity 500 instrument. Carbon-13 NMR spectra were recorded on either a Varian Unity 500 (at 125 MHz) or a Varian Unity Inova 400 (at 100 MHz) instrument. Negative-ion fast atom bombardment (FAB) mass spectra were recorded on a Kratos Concept 1S spectrometer (matrix *m*-nitrobenzyl alcohol); EPR spectra were recorded using either a Varian E112 or Bruker ESP 300E EPR spectrometer.

Cyclic voltammetric studies were performed on an EG&G PAR Model 362 Scanning Potentiostat with a Lloyds Instruments PL3 X-Y recorder. Either a glassy carbon or Pt wire working electrode, a Pt wire secondary electrode, a saturated calomel reference electrode (SCE) and the electrolyte $[NBu^n_4][PF_6]$[21] were used in the cell. Electrochemical potentials were measured relative to SCE in dimethylformamide (dmf) solution at room temperature, and under these conditions the $E_{\frac{1}{2}}$ for the $[FeCp_2]^+/[FeCp_2]$ (Cp = η-C_5H_5) couple was 487 mV and $\Delta E = 70$ mV.[22] Optically transparent thin-layer electrode (OTTLE)[23] measurements were obtained using a Varian Cary 1 spectrophotometer in conjunction with a Sycopel Scientific Ltd. DD10M potentiostat. A Pt–Rh gauze working electrode, a Pt wire secondary electrode, a SCE reference electrode and the electrolyte $[NBu^n_4][PF_6]$ were used in the cell. The initial voltages were chosen to be *ca.* 200 mV more negative than the $E_{\frac{1}{2}}$ value for the respective Mo^V–Mo^{IV} couple and the final voltage *ca.* 200 mV more positive, or until the spectrum no longer changed with increasingly positive potential. The applied potential was increased in 20 mV increments from the initial voltage. The reversibility of the system was confirmed by applying the initial potential after oxidation had been completed and reproducing the initial spectrum.

$[PPh_4]_2[MoO(sdt)_2]\cdot EtOH$ [sdt = $^-SC(H)C(C_6H_5)S^-$] 1a

The salt $K_4[MoO_2(CN)_4]\cdot 6H_2O$ (0.153 g, 0.31 mmol) and NaOH (0.099 g, 2.48 mmol) were dissolved in H_2O (5 cm^3) and addition of 2-(*N*,*N*-dimethylimino)-4-phenyl-1,3-dithiolium hydrogen sulfate (0.197 g, 0.62 mmol) in EtOH (5 cm^3) was followed by reflux (2 h) generating a red solution. Treatment of the hot reaction mixture with a solution of $[PPh_4]Cl$ (0.231 g, 0.62 mmol) and EtOH (5 cm^3) gave, on cooling, a red microcrystalline solid. The solid was separated by decantation of the mother-liquor, washed (H_2O, 15 cm^3) and dried *in vacuo.* Yield 0.121 g, 34% (Found: C, 67.87; H, 4.65; S, 11.12. Calc. for $C_{64}H_{52}MoOP_2S_4\cdot C_2H_6O$: C, 67.79; H, 5.00; S, 10.97%). ^1H NMR {300 MHz, $(CD_3)_2SO$ containing $Na[BH_4]$}: δ 8.09–7.80 (br, 44 H, $[PPh_4]^+$, H^2, H^6), 7.29 (m, 4 H, H^3, H^5), 7.20, 7.19 (2 × s, 2 × 1 H, $H_{dithiolene}$), 7.10 (m, 2 H, H^4). Mass spectrum (negative ion FAB): *m*/*z* 446 $[MoO(sdt)_2]^-$, 785 $[MoO(sdt)_2 + PPh_4]^-$.

The $[PBu^n_4]^+$ salt (**1b**) was prepared by a method similar to that used for the $[PPh_4]^+$ salt but using $[PBu^n_4]Br$. 4-Phenyl-1,3-dithiol-2-one was used as the ligand precursor and the product was isolated as an orange-red oil. ^1H NMR {500 MHz, $(CD_3)_2SO$ containing $[CoCp_2]$}: δ 7.77 (d, 4 H, H^2, H^6), 7.17 (m, 4 H, H^3, H^5), 7.13, 7.12 (2 × s, 2 × 1 H, $H_{dithiolene}$), 6.98 (m, 2 H, H^4), 2.06 (m, 16 H, $PCH_2CH_2CH_2CH_3$), 1.32 (m, 32 H, $PCH_2CH_2CH_2CH_3$), 0.83 (m, 24 H, $PCH_2CH_2CH_2CH_3$). ^{13}C NMR {125 MHz, $(CD_3)_2SO$ containing $[CoCp_2]$}: δ 144.27, 144.24, 142.94, 142.89 (C^1, $C^{1'}$), 130.06 ($C^{2'}$), 127.58 (C^3, C^5), 126.14 (C^2, C^6), 124.15 (C^4), 23.65, 23.52, 23.05, 23.01 ($PCH_2CH_2CH_2CH_3$), 17.84, 17.47 ($PCH_2CH_2CH_2CH_3$), 13.57 ($PCH_2CH_2CH_2CH_3$). Mass spectrum (negative ion FAB): *m*/*z* 446 $[MoO(sdt)_2]^-$, 705 $[MoO(sdt)_2 + PBu_4]^-$.

$[PPh_4]_2[MoO\{SC(D)C(C_6H_5)S\}_2]\cdot EtOH$ 1c

Sodium (0.089 g, 3.87 mmol) was dissolved in D_2O (5 cm^3) to give a solution of NaOD. The salt $K_4[MoO_2(CN)_4]\cdot 6H_2O$ (0.136 g, 0.27 mmol), 2-(*N*,*N*-dimethylimino)-4-phenyl-1,3-dithiolium hydrogensulfate (0.175 g, 0.55 mmol) and EtOD (5 cm^3) were added and the reaction mixture refluxed for 2 h. On cooling, the red solution was filtered and $[PPh_4]Cl$ (0.205 g, 0.55 mmol) added resulting in the precipitation of an orange-red solid. The product was separated by decantation of the mother-liquor, washed (D_2O, 2 × 6 cm^3) and dried *in vacuo.* Yield 0.101 g, 31%. ^1H NMR {300 MHz, $(CD_3)_2SO$ containing $Na[BH_4]$}: δ 8.09–7.80 (m, 44 H, $[PPh_4]^+$, H^2, H^6), 7.28 (m, 4 H, H^3, H^5), 7.09 (m, 2 H, H^4). Mass spectrum (negative ion FAB): *m*/*z* 448 $[MoO\{SC(D)C(C_6H_5)S\}_2]^-$, 787 $[MoO\{SC(D)C(C_6H_5)S\}_2 + PPh_4]^-$.

$[PPh_4]_2[MoO(2\text{-pedt})_2]$ {2-pedt = $^-SC(H)C[(C_5H_4N)\text{-}2]S^-$} 2a

Method A. The salt $K_4[MoO_2(CN)_4]\cdot 6H_2O$ (0.156 g, 0.31 mmol) and NaOH (0.113 g, 2.82 mmol) were dissolved in H_2O (5 cm^3). Addition of 4-(pyridin-2-yl)-1,3-dithiol-2-one (0.123 g, 0.63 mmol) and EtOH (5 cm^3) followed by reflux (2 h) generated a red solution. A solution of $[PPh_4]Cl$ (0.233 g, 0.62 mmol) in EtOH (2 cm^3) was added to the hot reaction mixture. Cooling and the addition of H_2O gave an oily residue which, on prolonged stirring, generated an orange solid. The solid was separated by decantation of the mother-liquor, washed (H_2O, 2 × 10 cm^3) and dried *in vacuo.* Yield 0.210 g, 59% (Found: C, 62.04; H, 5.00; N, 2.56; S, 9.29. Calc. for $C_{62}H_{50}MoN_2OP_2S_4$: C, 66.18; H, 4.48; N, 2.49; S, 11.40%).

Method B. 4-(Pyridin-2-yl)-1,3-dithiol-2-one (0.031 g, 0.16 mmol) was added, with stirring, to a solution of $CsOH\cdot H_2O$ (0.055 g, 0.33 mmol) in anhydrous MeOH (3 cm^3). After 10 min a solution of $K_4[MoO_2(CN)_4]\cdot 6H_2O$ (0.040 g, 0.08 mmol) in H_2O (3 cm^3) was added dropwise and the reaction mixture stirred for 1 h. The reaction mixture was then evaporated to dryness *in vacuo* giving a red residue. Extraction into H_2O (5 cm^3) and the dropwise addition of a solution of $[PPh_4]Cl$ (0.060 g, 0.16 mmol) in H_2O (2 cm^3) gave an orange solid. The solid was separated by decantation of the mother-liquor, washed (H_2O, 2 × 10 cm^3) and dried *in vacuo.* The product was recrystallised from EtOH to give $[PPh_4]_2[MoO(2\text{-pedt})_2]\cdot EtOH$ as a red solid. Yield 0.017 g, 18% (Found: C, 65.42; H, 4.53; N, 2.71; S, 11.58. Calc. for $C_{62}H_{50}MoN_2OP_2S_4\cdot C_2H_6O$: C, 65.63; H, 4.82; N, 2.39; S, 10.95%). ^1H NMR {300 MHz, $(CD_3)_2SO$ containing $Na[BH_4]$}: δ 8.29 (m, 2 H, H^6), 8.02 (m, 2 H, H^3), 7.95–7.66 (m, 42 H, $[PPh_4]^+$, $H_{dithiolene}$), 7.58 (m, 2 H, H^4), 6.91 (m, 2 H, H^5). Mass spectrum (negative ion FAB): *m*/*z* 448 $[MoO(2\text{-pedt})_2]^-$, 787 $[MoO(2\text{-pedt})_2 + PPh_4]^-$.

The $[PBu^n_4]^+$ salt (**2b**) was prepared in a similar manner to that of the $[PPh_4]^+$ salt from $[PBu^n_4]Br$. ^1H NMR {400 MHz, $(CD_3)_2SO$ containing $Na[BH_4]$}: δ 8.33 (m, 2 H, H^6), 8.07 (m, 2 H, H^3), 7.96, 7.95 (2 × s, 2 × 1 H, $H_{dithiolene}$), 7.61 (m, 2 H, H^4), 6.94 (m, 2 H, H^5), 2.10 (m, 16 H, $PCH_2CH_2CH_2CH_3$), 1.34 (m, 32 H, $PCH_2C\mathit{H}_2C\mathit{H}_2CH_3$), 0.86 (m, 24 H, $PCH_2CH_2CH_2C\mathit{H}_3$). ^{13}C NMR {100 MHz, $(CD_3)_2SO$ containing $Na[BH_4]$}: δ 159.10 (C-2), 148.42 (C-6), 144.75, 144.66 (C-1′), 136.21, 136.11 (C-2′), 136.00 (C-4), 119.70 (C-3), 119.17 (C-5), 23.88, 23.73, 23.20, 23.15 ($PCH_2\mathit{C}H_2\mathit{C}H_2CH_3$), 18.05, 17.58 ($P\mathit{C}H_2CH_2CH_2CH_3$), 13.77 ($PCH_2CH_2CH_2\mathit{C}H_3$). Mass spectrum (negative ion FAB): *m/z* 448 $[MoO(2\text{-}pedt)_2]^-$, 707 $[MoO(2\text{-}pedt)_2 + PBu_4]^-$.

$[PPh_4]_2[MoO(3\text{-}pedt)_2]\cdot EtOH$ {3-pedt = $^-SC(H)C[(C_5H_4N)\text{-}3]S^-$} 3a

This compound was prepared as for **1a** from $K_4[MoO_2(CN)_4]\cdot 6H_2O$ (0.135 g, 0.27 mmol), NaOH (0.138 g, 3.45 mmol), 2-(*N*,*N*-dimethylimino)-4-(pyridin-3-yl)-1,3-dithiolium hydrogensulfate (0.174 g, 0.55 mmol) and $[PPh_4]Cl$ (0.203 g, 0.54 mmol). The product was isolated as a red-brown solid. Yield 0.125 g, 39% (Found: C, 64.86; H, 4.78; N, 2.61; S, 10.80. Calc. for $C_{62}H_{50}MoN_2OP_2S_4\cdot C_2H_6O$: C, 65.63; H, 4.82; N, 2.39; S, 10.95%).

Solvent free $[PPh_4]_2[MoO(3\text{-}pedt)_2]$ was also prepared as for **1a** from $K_4[MoO_2(CN)_4]\cdot 6H_2O$ (0.056 g, 0.11 mmol), NaOH (0.060 g, 1.50 mmol), 4-(pyridin-3-yl)-1,3-dithiol-2-one (0.043 g, 0.22 mmol) and $[PPh_4]Cl$ (0.085 g, 0.23 mmol). Yield 0.067 g, 53% (Found: C, 65.19; H, 4.56; N, 2.49; S, 11.34. Calc. for $C_{62}H_{50}MoN_2OP_2S_4$: C, 66.18; H, 4.48; N, 2.49; S, 11.40%). ^1H NMR {300 MHz, $(CD_3)_2SO$]: δ 8.93 (m, 2 H, H^2), 8.18 (m, 2 H, H^6), 8.06 (m, 2 H, H^4), 7.97–7.68 (m, 40 H, $[PPh_4]^+$), 7.24, 7.23 (2 × s, 2 × 1 H, $H_{dithiolene}$), 7.19 (m, 2 H, H^5). Mass spectrum (negative ion FAB): *m/z* 447 $[MoO(3\text{-}pedt)_2]^-$, 787 $[MoO(3\text{-}pedt)_2 + PPh_4]^-$.

The $[PBu^n{}_4]^+$ salt (**3b**) was prepared by a similar method to that of the $[PPh_4]^+$ salt from $[PBu^n{}_4]Br$. 4-(Pyridin-3-yl)-1,3-dithiol-2-one was used as the ligand precursor and the product was isolated as an orange-red oil. ^1H NMR [300 MHz, $(CD_3)_2SO$]: δ 8.94 (m, 2 H, H^2), 8.17 (m, 2 H, H^6), 8.07 (m, 2 H, H^4), 7.27, 7.26 (2 × s, 2 × 1 H, $H_{dithiolene}$), 7.19 (m, 2 H, H^5), 2.08 (m, 16 H, $PC\mathit{H}_2CH_2CH_2CH_3$), 1.32 (m, 32 H, $PCH_2C\mathit{H}_2C\mathit{H}_2CH_3$), 0.83 (m, 24 H, $PCH_2CH_2CH_2C\mathit{H}_3$). Mass spectrum (negative ion FAB): *m/z* 448 $[MoO(3\text{-}pedt)_2]^-$, 707 $[MoO(3\text{-}pedt)_2 + PBu_4]^-$.

$[PPh_4]_2[MoO(4\text{-}pedt)_2]$ {4-pedt = $^-SC(H)C[(C_5H_4N)\text{-}4]S^-$} 4a

This compound was prepared as for **1a** using $K_4[MoO_2(CN)_4]\cdot 6H_2O$ (0.144 g, 0.29 mmol), NaOH (0.142 g, 3.60 mmol) and 2-(*N*,*N*-dimethylimino)-4-(pyridin-4-yl)-1,3-dithiolium hydrogensulfate (0.186 g, 0.58 mmol). Addition of $[PPh_4]Cl$ (0.217 g, 0.58 mmol) to the reaction mixture precipitated the product as an orange-brown solid which was separated by filtration, washed (H_2O_2, 2 × 15 cm^3, then Et_2O, 10 cm^3) and dried *in vacuo.* Yield 0.095 g, 29% (Found: C, 64.84; H, 4.60; N, 2.42; S, 11.12. Calc. for $C_{62}H_{50}MoN_2OP_2S_4$: C, 66.18; H, 4.48; N, 2.49; S, 11.40%).

The compound $[PPh_4]_2[MoO(4\text{-}pedt)_2]\cdot EtOH$ was also prepared as in Method B for $[PPh_4]_2[MoO(2\text{-}pedt)_2]$ using 4-(pyridin-4-yl)-1,3-dithiol-2-one (0.029 g, 0.15 mmol), $CsOH\cdot H_2O$ (0.052 g, 0.31 mmol), $K_4[MoO_2(CN)_4]\cdot 6H_2O$ (0.038 g, 0.08 mmol) and $[PPh_4]Cl$ (0.057 g, 0.15 mmol). The product was recrystallised from absolute EtOH as a dark red microcrystalline solid. Yield 0.030 g, 33.5% (Found: C, 65.38; H, 4.56; N, 2.40; S, 10.75. Calc. for $C_{62}H_{50}MoN_2OP_2S_4\cdot C_2H_6O$: C, 65.63; H, 4.82; N, 2.39; S, 10.95%). ^1H NMR {300 MHz, $(CD_3)_2SO$ containing $Na[BH_4]$}: δ 8.26 (m, 4 H, H^2, H^6), 7.95–7.66 (m, 44 H, $[PPh_4]^+$, H^3, H^5), 7.55, 7.53 (2 × s, 2 × 1 H, $H_{dithiolene}$). Mass spectrum (negative ion FAB): *m/z* 448 $[MoO(4\text{-}pedt)_2]^-$, 787 $[MoO(4\text{-}pedt)_2 + PPh_4]^-$.

The $[PBu^n{}_4]^+$ salt (**4b**) was prepared by a similar method to that for the $[PPh_4]^+$ salt from $[PBu^n{}_4]Br$. 4-(Pyridin-4-yl)-1,3-dithiol-2-one was used as the ligand precursor and the product was isolated as a dark red oil. ^1H NMR {400 MHz, $(CD_3)_2SO$ containing $Na[BH_4]$}: δ 8.28 (m, 4 H, H^2, H^6), 7.72 (m, 4 H, H^3, H^5), 7.60, 7.58 (2 × s, 2 × 1 H, $H_{dithiolene}$), 2.05 (m, 16 H, $PC\mathit{H}_2CH_2CH_2CH_3$), 1.32 (m, 32 H, $PCH_2C\mathit{H}_2C\mathit{H}_2CH_3$), 0.82 (m, 24 H, $PCH_2CH_2CH_2C\mathit{H}_3$). Mass spectrum (negative ion FAB): *m/z* 448 $[MoO(4\text{-}pedt)_2]^-$, 707 $[MoO(4\text{-}pedt)_2 + PBu_4]^-$.

$[PPh_4]_2[MoO(qedt)_2]$ [qedt = $^-SC(H)C(C_6H_4N_2C_2H)S^-$] 5a

The salt $K_4[MoO_2(CN)_4]\cdot 6H_2O$ (0.086 g, 0.17 mmol) and NaOH (0.144 g, 3.60 mmol) were dissolved in H_2O (5 cm^3). Addition of 2-(*N*,*N*-dimethylimino)-4-(quinoxalin-2-yl)-1,3-dithiolium hydrogensulfate (0.128 g, 0.34 mmol) in EtOH (5 cm^3) gave a red solution. The reaction mixture was refluxed for 1 h generating a dark red solution, which was cooled and filtered before a solution of $[PPh_4]Cl$ (0.062 g, 0.17 mmol) in EtOH (2 cm^3) was added. Treatment with H_2O (15 cm^3) resulted in the precipitation of a red-purple solid. Purification was achieved by reprecipitation of the product from an acetone solution by addition of Et_2O. Yield 0.036 g, 17% (Found: C, 65.08; H, 4.40; N, 4.36; S, 10.67. Calc. for $C_{68}H_{52}MoN_4OP_2S_4$: C, 66.55; H, 4.27; N, 4.57; S, 10.45%). ^1H NMR [300 MHz, $(CD_3)_2SO$]: δ 9.78, 9.75 (2 × s, 2 × H, H^3), 8.41, 8.40 (2 × s, 2 × 1 H, $H_{dithiolene}$), 8.08–7.78 (m, 46 H, $[PPh_4]^+$, H^5, H^8, H^6/H^7), 7.71 (m, 2 H, H^6/H^7). Mass spectrum (negative ion FAB): *m/z* 550 $[MoO(qedt)_2]^-$.

The $[PBu^n{}_4]^+$ salt (**5b**) was prepared by a similar method to that for the $[PPh_4]^+$ salt from $[PBu^n{}_4]Br$. 4-(Quinoxalin-2-yl)-1,3-dithiol-2-one was used as the ligand precursor and the product was isolated as a red-purple oil. ^1H NMR [300 MHz, $(CD_3)_2SO$]: δ 9.82, 9.79 (2 × s, 2 × 1 H, H^3), 8.46, 8.44 (2 × s, 2 × 1 H, $H_{dithiolene}$), 8.03 (m, 4 H, H^5, H^8), 7.83 (m, 2 H, H^6/H^7), 7.72 (m, 2 H, H^6/H^7), 2.21 (m, 16 H, $PC\mathit{H}_2CH_2CH_2CH_3$), 1.44 (m, 32 H, $PCH_2C\mathit{H}_2C\mathit{H}_2CH_3$), 0.95 (m, 24 H, $PCH_2CH_2CH_2C\mathit{H}_3$). ^{13}C NMR {125 MHz, $DCON(CD_3)_2$ containing $[CoCp_2]$}: δ 152.72 (C^2), 145.23, 145.21 (C^3), 142.83, 142.66 ($C^{1'}$), 142.59, 142.43 ($C^{2'}$), 141.87, 139.74 (C^9, C^{10}), 128.74 (C^6/C^7), 128.10, 127.99 (C^5, C^8), 126.16 (C^6/C^7), 23.14, 23.02, 22.66, 22.63 ($PCH_2\mathit{C}H_2\mathit{C}H_2CH_3$), 17.52, 17.14 ($P\mathit{C}H_2CH_2CH_2CH_3$), 12.36 ($PCH_2CH_2CH_2\mathit{C}H_3$). Mass spectrum (negative ion FAB): *m/z* 550 $[MoO(qedt)_2]^-$, 809 $[MoO(qedt)_2 + PBu_4]^-$.

$K[PPh_4][MoO(NH_2\text{-}ptedt)_2]$ {NH_2-ptedt = $^-SC(H)C[N(H_2N)CN(Me)C(O)C_2N_2C_2]S^-$} 6a

The salt $K_4[MoO_2(CN)_4]\cdot 6H_2O$ (0.022 g, 0.04 mmol) and NaOH (0.012 g, 0.30 mmol) were dissolved in H_2O (5 cm^3). 4-(2-*N*,*N*-Dimethylaminomethyleneamino)-3-methyl-4-oxopteridin-6-yl-1,3-dithiol-2-one (0.030 g, 0.09 mmol) and EtOH (5 cm^3) were added and the reaction mixture refluxed for 45 min generating a dark red solution. Addition of $[PPh_4]Cl$ (0.078 g, 0.21 mmol) to the hot solution gave, on cooling and the addition of H_2O (5 cm^3), a red solid. The solid was separated by filtration, washed (H_2O, 2 × 5 cm^3) and dried *in vacuo.* Yield 0.027 g, 60% (Found: C, 50.06; H, 3.96; N, 10.76; S, 7.76. Calc. for $C_{42}H_{34}KMoN_{10}O_3PS_4$: C, 49.40; H, 3.36; N, 13.72; S, 12.56%). ^1H NMR [300 MHz, $(CD_3)_2SO$]: δ 9.50, 9.49 (2 × s, 2 × 1 H, H^7), 8.09–7.81 (m, 22 H, $[PPh_4]^+$, $H_{dithiolene}$), 7.41 (br, 4 H, NH_2), 3.52 (s, 6 H, NCH_3). Mass spectrum (electrospray): *m/z* 644 $[MoO(NH_2\text{-}ptedt)_2]^-$.

$K_2[MoO(NH_2\text{-}ptedt)_2]$ 6b

This was prepared essentially as described for salt **6a** (Found: C, 30.41; H, 2.16; N, 16.30; S, 14.63. Calc. for $C_{18}H_{14}K_2MoN_{10}O_3S_4$: C, 30.00; H, 1.96; N, 19.44; S, 17.79%). ^1H NMR [400 MHz, $(CD_3)_2SO$]: δ 9.37, 9.36 (2 × s, 2 × 1 H, H^7), 7.91, 7.90 (2 × s, 2 × 1 H, $H_{dithiolene}$), 7.29 (br, 4 H, NH_2), 3.38 (s, 6 H, NCH_3). Mass spectrum (negative ion FAB): *m/z* 653 $[Mo(NH_2\text{-}ptedt)_2 + K - CH_3]^-$, 636 $[Mo(NH_2\text{-}ptedt)_2 + K - 2CH_3]^-$.

Table 1 Structure analysis of complex **1a**

Formula	$C_{66}H_{58}MoO_2P_2S_4$
M	1169.31
Colour	Red
Crystal system	Monoclinic
Space group	$P2_1/c$ (no. 14)
a/Å	13.217(4)
b/Å	31.820(8)
c/Å	14.534(7)
β/°	113.8(2)
U/Å^3	5598(4)
Z	4
T/K	293
D_c/g cm^{-3}	1.387
F(000)	2424
μ(Mo-Kα)/cm^{-1}	4.71
Diffractometer	Rigaku AFC5R
Crystal dimensions/mm	0.05 × 0.15 × 0.28
λ(Mo-Kα)/Å	0.710 69
θ_{max}/°	25.05
Scan type	ω
Scan width	0.80 + 0.30 tan θ
Total data	10 600
Unique data	10 141
'Observed' data [$I > 3\sigma(I)$], N_o	5259
Least square variables, N_v	676
R*	0.057
R'*	0.053
S*	1.61
Difference map features/e Å^{-3}	0.67, −0.74

* $R = \Sigma||F_o| - |F_c||/\Sigma|F_o|$, $R' = [\Sigma w(|F_o| - |F_c|)^2/\Sigma wF_o^2]^{\frac{1}{2}}$, $S = [\Sigma w(|F_o| - |F_c|)^2/(N_o - N_v)]^{\frac{1}{2}}$.

$[PPh_4]_2[MoO\{NC(H)N(Me)_2\text{-ptedt}\}_2]$ $\{NC(H)N(Me)_2\text{-ptedt} = {}^-SC(H)C[N(Me_2NCN)CN(Me)C(O)C_2N_2C_2]S^-\}$ 7

4-(2-*N*,*N*-Dimethylaminomethyleneamino)-3-methyl-4-oxopteridin-6-yl-1,3-dithiol-2-one (0.035 g, 0.10 mmol) was added, with stirring, to a solution of $CsOH\cdot H_2O$ (0.035 g, 0.21 mmol) in 1 : 1 $CHCl_2$–MeOH (4 cm^3). After 12 min the resultant red-brown solution was evaporated to dryness *in vacuo.* The residue was dissolved in MeOH (3 cm^3) and a solution of $K_4[MoO_2(CN)_4]\cdot 6H_2O$ (0.025 g, 0.05 mmol) in H_2O (3 cm^3) added. The reaction mixture was stirred for 1 h before being evaporated to dryness. Extraction into H_2O (12 cm^3) and filtration followed by the addition of $[PPh_4]Cl$ (0.051 g, 0.14 mmol) resulted in the precipitation of a red-brown solid. The solid was separated by decantation of the mother-liquor, washed (H_2O, 2 × 10 cm^3) and dried *in vacuo.* Yield 0.033 g, 46% (Found: C, 60.21; H, 4.00; N, 11.24; S, 9.13. Calc. for $C_{72}H_{64}MoN_{12}O_3P_2S_4$: C, 60.41; H, 4.51; N, 11.74; S, 8.96%). ^1H NMR {300 MHz, $(CD_3)_2SO$ containing $Na[BH_4]$}: δ 9.46 (s, 2 H, H^7), 8.75 (s, 2 H, NC*H*NMe$_2$), 8.08, 8.06 (2 × s, 2 × 1 H, $H_{dithiolene}$), 7.96–7.68 (m, 40 H, $[PPh_4]^+$), 3.55 (s, 6 H, NCH_3), 3.23 (s, 6 H, NCHN*Me*$_2$), 3.11 (s, 6 H, NCHN*Me*$_2$). Mass spectrum (negative ion FAB): *m*/*z* 754 $[MoO\{NC(H)N(Me)_2\text{-ptedt}\}_2]^-$.

Crystallography

Red crystals of complex **1a** were grown by the slow diffusion of an ethanolic solution of $[PPh_4]Cl$ into a reaction mixture, prepared as for **1a**. The crystals were small and weakly diffracting. The one used for data collection had dimensions 0.05 × 0.15 × 0.28 mm. Minimal decay (−1.10% decline) suggested that the capillary-mounted crystals remained stable during data collection and hence oxidation was negligible. Details of the unit cell, data collection and refinement are given in Table 1. Data were collected on a Rigaku AFC5R diffractometer with graphite-monochromated Mo-Kα radiation and a 12 kW rotating anode generator at room temperature using the ω scanning technique. The data were corrected for Lorentz and polarisation effects and absorption using the DIFABS program.[24] The intensities of three representative reflections were measured after every 150 reflections and a linear correction factor was included to account for the observed decay. The structure was solved by direct methods.[25] Non-hydrogen atoms were refined anisotropically; hydrogen atoms were included in the structure factor with all C–H = 0.95 Å, and were assigned isotropic thermal parameters which were 20% greater than the equivalent B value of the atom to which they were bound. The function minimised during least-squares refinement was $\Sigma w(|F_o| - |F_c|)^2$ using standard neutral atom dispersion factors and anomalous dispersion corrections.[26,27] All calculations were performed using the TEXSAN[28] crystallographic package. Least-squares planes were calculated using the PLATON program.[29]

CCDC reference number 186/628.

Results

Synthesis

The total synthesis of Moco required that, as first step, we developed a general strategy for the synthesis of unsymmetrical ene–1,2-ditholate (dithiolene) ligands. Before our work, the chemistry of dithiolene complexes has primarily involved symmetrical ligands.[30] Given the general sensitivity of the ene–1,2-dithiolate groups, another key element in our synthetic strategy was the protection of this functionality until delivery to the metal. The feasibility of this approach was demonstrated by the synthesis of three tris(dithiolene) metalate complexes, $[M(sdt)_3]^{n-}$ [M = V, n = 1; M = Mo, n = 0; M = W, n = 0; sdt = 2-phenylethene-1,2-dithiolate (styrene-1,2-dithiolate)] by the alkaline hydrolysis of 2-(*N*,*N*-dimethylimino)-4-phenyl-1,3-dithiolium hydrogensulfate in the presence of $VOSO_4\cdot 3H_2O$, $[MoO_2(acac)_2]$ (acac = pentane-2,4-dionate), or WCl_6, respectively.[31]

This paper describes two important and further developments of this strategy. First, the identification of a range of precursors to dithiolene ligands $^-S(R)C{=}C(H)S^-$ [where R = Ph, pyridin-2-yl, pyridin-3-yl, pyridin-4-yl, quinoxalin-2-yl or 2-(dimethylaminomethyleneamino)-3-methyl-4-oxopteridin-6-yl]. Secondly, use of *trans*-$[MoO_2(CN)_4]^{4-}$ as the initial form of the molybdenum has allowed the preparation of $[MoO\{S(H)C{=}C(R)S\}_2]^{2-}$ complexes, rather than the tris-complexes described previously.[31] Oxobis(dithiolene)molybdenum complexes are directly relevant to the active centre of the oxomolybdoenzymes which involve two mpt units per Mo, *e.g.* DMSO reductase[11–13] and formate dehydrogenase H.[14]

A series of dimethylamino- or thione-protected 1,3-dithiolates have been synthesised[18–20] from the corresponding bromoacetyl moiety by one of the two routes shown in Scheme 1. Addition of alkali to these protected dithiolenes, either as the 1,3-dithiol-2-one or the 1,3-dithiol-2-iminium salt in aqueous EtOH generated the corresponding ethene-1,2-dithiolate. For the pterin-containing proligand hydrolysis was carried out in MeOH–$CHCl_3$ to aid solubility and it is noted that in the synthesis of **6**, where excess base was employed, hydrolysis of the dimethylaminomethylene protecting group at C^2 also occurred. The dithiolenes were not isolated since they were unstable, so hydrolysis was carried out either immediately prior to the addition of *trans*-$[MoO_2(CN)_4]^{4-}$ to the reaction solution or in the presence of this complex. Ligand substitution at the molybdenum centre was achieved either by stirring at room temperature or by refluxing the reaction mixture (Scheme 2). The use of alkaline hydrolysis to achieve the deprotection of the dithiolene also avoided protonation and subsequent loss of both oxo groups from $[MoO_2(CN)_4]^{4-}$. We suggest that the high H^+ concentration of the reaction mixtures used previously probably accounts for the formation of tris-dithiolene complexes from $[MoO_2(acac)_2]$, since acidification was employed to protonate the pentane-2,4-dionate prior to its substitution.[31] The

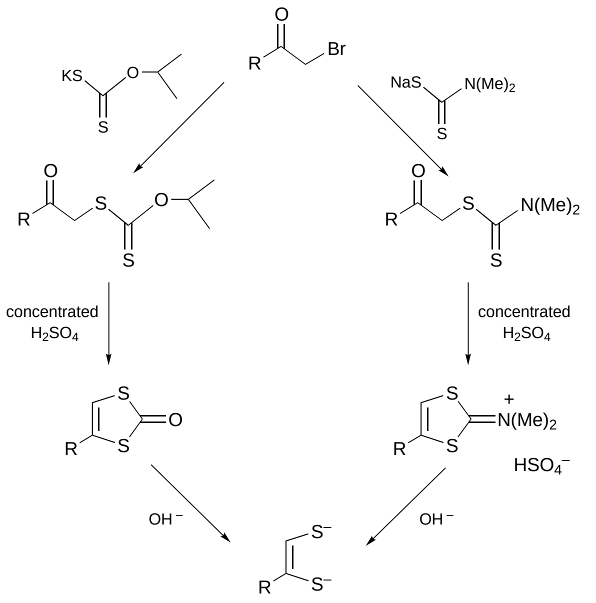

Scheme 1

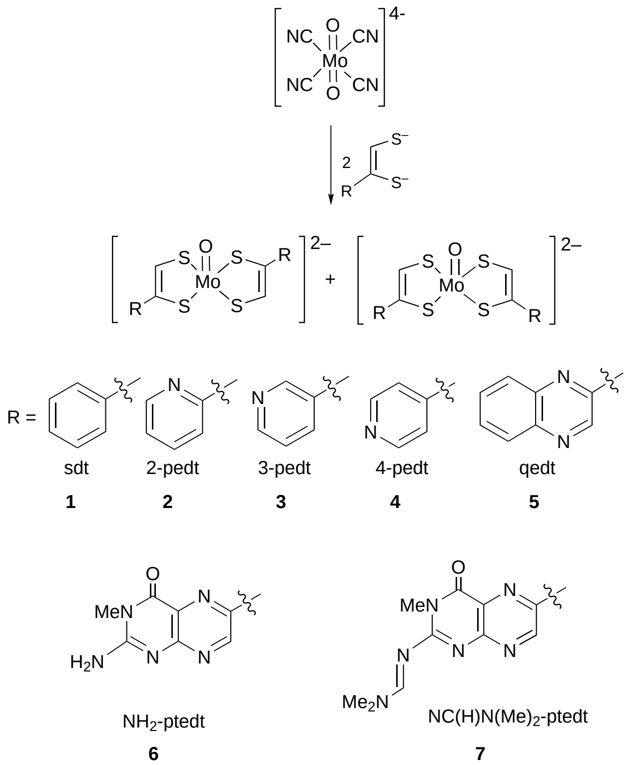

Scheme 2

$[MoO(dithiolene)_2]^{2-}$ complexes thus generated were isolated by the addition of 2 equivalents of $[PR_4]X$ (R = Ph, X = Cl or R = Bu^n, X = Br). The formal oxidation state of the metal centre in $[MoO(dithiolene)_2]^{2-}$ as Mo^{IV} was retained from that in the starting material.

The products were isolated, in the case of $[PPh_4]^+$ salts, as red (sdt), red-brown (pterins), orange-brown (2-pedt, 3-pedt, 4-pedt) or red-purple (qedt) solids. In the case of the $[PBu^n_4]^+$ salts, prepared for the unobstructed examination of the aromatic region in the ^{1}H NMR spectra, the products were isolated as oils. All of the compounds rapidly discoloured to brown on exposure to air. Solutions became orange-yellow on standing in air and developed strong EPR signals characteristic of Mo^VOS_4 centres (see below). The complexes were stable in the presence of alkali but acidic solutions became green and the addition of CF_3CO_2H to $[MoO(sdt)_2]^{2-}$ in dmso was shown to produce $[Mo(sdt)_3]$.

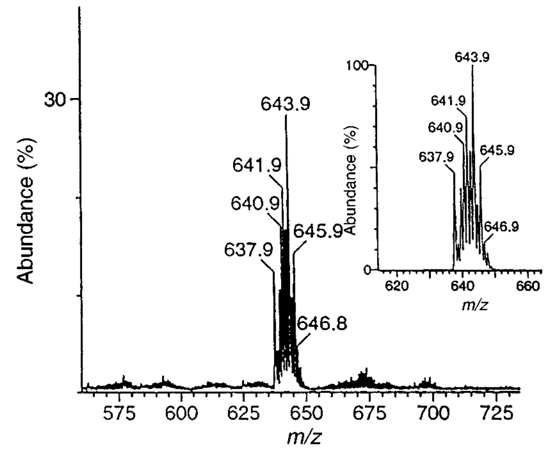

Fig. 2 Electrospray mass spectrum of complex **6a** at the molecular ion region and the calculated isotopic distribution pattern (inset)

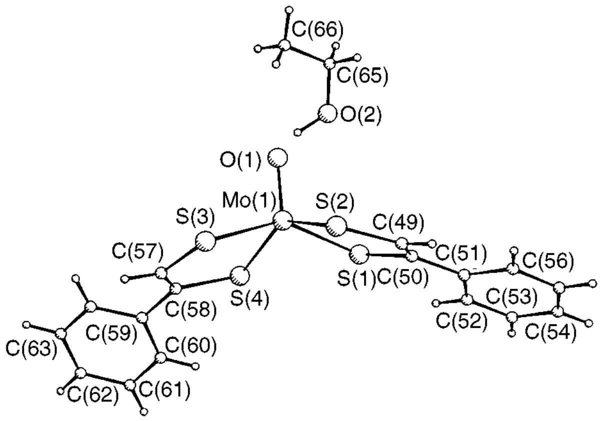

Fig. 3 Molecular structure of the dianion of **1a** showing the ethanol of crystallisation as drawn by PLUTO[32]

Characterisation

Analysis. Although the agreement between the experimental analytical data and the expected values was generally good, we note the relatively poor agreement between calculated and observed values for N and S in compounds **6a** and **6b**. However, all of the spectroscopic data on these compounds were consistent with the presence of $[MoO(dithiolene)_2]^{2-}$ with no other molybdenum–dithiolene containing species being present.

Mass spectrometry. Mass spectrometry proved particularly valuable for the identification of these $[MoO(dithiolene)_2]^{2-}$ complexes. A series of peaks with the characteristic Mo isotope distribution were observed at *m*/*z* values corresponding to $[MoO(dithiolene)_2]^-$ in the negative ion FAB spectra; for **6a**, we employed electrospray mass spectrometry (Fig. 2). The Mo isotopic distribution at *m*/*z* values corresponding to $[MoO(dithiolene)_2 + PR_4]^-$ (R = Ph or Bu^n) were also observed in most of the spectra.

Crystallography. The structure of the $[MoO(sdt)_2]^{2-}$ anion of **1** is illustrated in Fig. 3 and selected bond distances and angles are listed in Table 2.

The $MoOS_4$ centre has a square-based pyramidal structure with the O atom at the apex; the Mo atom is raised above the basal plane by 0.78 Å and the mean deviation of S atoms from the basal plane is 0.05 Å. The phenyl groups of the styrenedithiolate ligands are located on the same side of the square base and this we define as the *cis* isomer. The *trans* isomer was not observed in the single crystal X-ray diffraction analysis of **1a**. The Mo=O bond distance of 1.700(5) Å is slightly longer

Table 2 Selected bond distances (Å), bond angles (°) amd torsion angles (°) of $[PPh_4]_2[MoO(sdt)_2]{\cdot}EtOH$

Mo(1)–O(1)	1.700(5)	C(49)–C(50)	1.33(1)
Mo(1)–S(1)	2.366(2)	C(57)–C(58)	1.325(9)
Mo(1)–S(2)	2.376(2)	S(1)–C(50)	1.773(7)
Mo(1)–S(3)	2.385(2)	S(2)–C(49)	1.751(8)
Mo(1)–S(4)	2.370(2)	S(3)–C(57)	1.738(8)
		S(4)–C(58)	1.774(7)
O(1)–Mo(1)–S(1)	107.5(2)	Mo(1)–S(1)–C(50)	108.2(3)
O(1)–Mo(1)–S(2)	110.3(2)	Mo(1)–S(2)–C(49)	106.6(3)
O(1)–Mo(1)–S(3)	107.9(2)	Mo(1)–S(3)–C(57)	106.7(3)
O(1)–Mo(1)–S(4)	110.7(2)	Mo(1)–S(4)–C(58)	107.7(3)
S(1)–Mo(1)–S(2)	82.68(7)	S(1)–C(50)–C(49)	118.5(6)
S(2)–Mo(1)–S(3)	86.92(7)	S(2)–C(49)–C(50)	123.2(6)
S(3)–Mo(1)–S(4)	82.17(7)	S(3)–C(57)–C(58)	112.8(6)
S(1)–Mo(1)–S(4)	83.78(7)	S(4)–C(58)–C(57)	118.9(6)
C(49)–C(50)–C(51)–C(52)	162.0(8)		
C(49)–C(50)–C(51)–C(56)	−18(1)		
C(57)–C(58)–C(59)–C(60)	−135.9(8)		
C(57)–C(58)–C(59)–C(64)	43(1)		

than that found in other Mo^{IV} complexes containing the $MoOS_4$ motif $\{[MoO(bdt)_2]^{2-}$ (bdt = benzene-1,2-dithiolate), 1.668(3) Å;[33] $[MoO(mnt)_2]^{2-}$ (mnt = 1,2-dicyanoethylene-dithiolate), 1.67(1) Å[34]$\}$. A mean Mo–S bond length of 2.37 Å is consistent with the corresponding bond lengths in $[MoO(mnt)_2]^{2-}$ (2.38 Å) and $[MoO(bdt)_2]^{2-}$ (2.38 Å). The C=C bond length of 1.33 Å in **1** is similar to those in $[MoO(mnt)_2]^{2-}$ (1.35 Å) and $[MoCp_2(qedt)]$ (1.34 Å)[35] and the mean O–Mo–S inter-bond angle of 109.1° for **1** is similar to that in $[MoO(bdt)_2]^{2-}$ (108.1°).

The two, five-membered metallocycles, defined by Mo(1)–S(1)–S(2)–C(49)–C(50) and Mo(1)–S(3)–S(4)–C(57)–C(58), are essentially planar (with a mean deviation from the planes of 0.08 and 0.11 Å, respectively) and subtend a dihedral angle of 49.2° within the anion. The EtOH of crystallisation is outside the co-ordination sphere of the Mo but appears to be hydrogen bonded to O(1) [O(1)–O(2) 2.85(1) Å] (see Fig. 3). The $[PPh_4]^+$ counter ions are structurally unremarkable.

Proton and ^{13}C NMR spectroscopy. The air-sensitive nature of the compounds resulted in slight oxidation of the products during synthesis and/or sample preparation for spectroscopic study. The extent of this sensitivity correlated with the $E_{\frac{1}{2}}$ value of the Mo^V–Mo^{IV} couple (see below). Trace amounts of Mo^V, probably as $[MoO(dithiolene)_2]^-$, resulted in a broadening of ^1H resonances associated with the ligands (although the resonances of the counter cations remained relatively well resolved). This effect was most pronounced for the dithiolene ^1H resonance, as might be expected since this is the proton closest to the source of paramagnetic activity, the Mo atom. The observation that only a small quantity of the Mo^V species produced this effect suggests the presence of an efficient electron exchange process between $[MoO(dithiolene)_2]^{2-}$ and $[MoO(dithiolene)_2]^-$ species. We observed that the addition of small quantities of a reductant (either $Na[BH_4]$ or $[CoCp_2]$) resulted in a ^1H NMR spectrum of the $[MoO(dithiolene)_2]^{2-}$ complex with complete resolution of all proton environments (see Fig. 4) (a similar effect was also observed for the ^{13}C NMR spectra). These reductants appeared to serve only to remove the Mo^V species and sharpen the ^1H (and ^{13}C) resonances without affecting their chemical shifts or multiplicity. For example, the ^1H NMR spectrum of **4a** in $(CD_3)_2SO$ (resolved without the requirement of reductant) showed ^1H resonances at δ 8.26, 7.95–7.66, 7.55 and 7.53. On addition of $Na[BH_4]$, the ligand proton resonances sharpened but no significant variance in chemical shift or multiplicity was observed (resonances: δ 8.27, 7.95–7.66, 7.55 and 7.53). Conversely, for **5** in $(CD_3)_2SO$ which manifested a well resolved ^1H NMR spectrum, addition of $[FeCp_2][PF_6]$ resulted in a broadening of the resonances of the quinoxalinyl protons and the complete loss of the dithiolene proton resonance.

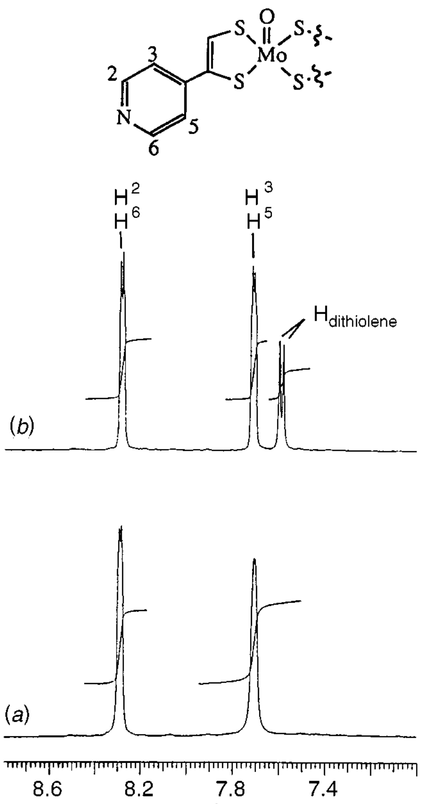

Fig. 4 The 300 MHz ^1H NMR spectra of complex **4b** in $(CD_3)_2SO$ in the aromatic region showing (*a*) partially oxidised and (*b*) $Na[BH_4]$ reduced samples

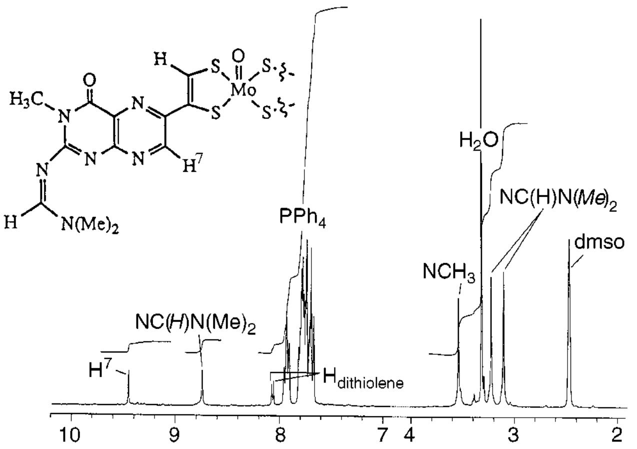

Fig. 5 The 300 MHz ^1H NMR spectrum of complex **7** in $(CD_3)_2SO$, reduced with $Na[BH_4]$

The presence of resonances due to EtOH in complexes **1**–**7** was dependent on the method of isolation and purification.

Apart from the ^1H resonances of EtOH and the cations, the use of $[PBu^n{}_4]^+$ was particularly helpful in allowing a clear view of the aromatic region, ^1H resonances for the $[MoO(dithiolene)_2]^{2-}$ complexes were observed in the following regions: δ 7.13–8.50 ($H_{dithiolene}$) and 6.91–9.78 ($H_{aromatic/heteroaromatic}$), the former being dependent upon the nature of the R group. A prototypical spectrum, that of **7**, containing the biologically relevant pterin ligand, is shown in Fig. 5. In addition to the dithiolene and heteroaromatic ^1H resonances, the spectrum also includes methyl resonances derived from the protecting groups at C^2 and N^3.

In general, the chemical shifts of the ligand resonances in the

^{1}H NMR spectra of complexes **1**–**7** are consistent with those reported for other complexes of Mo^{IV} with asymmetric dithiolene ligands.[35] However, in contrast to these pseudo-tetrahedral [MoCp$_2$(dithiolene)] complexes, the presence of two asymmetric dithiolenes in a square-pyramidal geometry of MoOS_4 allows the formation of *cis* and *trans* isomers. The structure of **1a** indicates an exclusively *cis* orientation, however, it is expected that the syntheses would produce a 1 : 1 mixture of isomers. The ^{1}H NMR spectra of these complexes indicated the presence of both isomeric forms, especially for the environments of the ene fragment. Thus, the ^{1}H NMR spectrum of all of the compounds showed two singlets for the dithiolene protons; the assignment as singlets was confirmed by a lack of coupling to these resonances in ^{1}H–^{1}H COSY and ^{1}H decoupling experiments. Also, the ratio of the integrals of the two singlets varied with the method of isolation of the compounds. For example, the preparation of **1b** produced an oil, the ^{1}H NMR spectrum of which contained resonances at δ 7.12 and 7.13 with essentially equal integrals. In contrast, a crystalline sample of **1a** gave a ^{1}H NMR spectrum with resonances at δ 7.19 and 7.20 but with an integral ratio of *ca.* 3 : 1; *i.e.* a preferential crystallisation of one isomer was achieved and, given the crystal structure result (see Fig. 2), the resonance at δ 7.19 is attributed to the *cis* isomer. A similar effect was observed for **4a**, where recrystallisation from EtOH led to the isolation of a product in which the relative integrals of the dithiolene ^{1}H resonance at δ 7.53 and 7.55 was *ca.* 6 : 1.

The ^{13}C NMR spectra of **1b**, **2b** and **5b** were recorded and each showed two environments for the quaternary carbons (C^1 and C$^{1'}$ in **1b**, C$^{1'}$ in **2b** and C^2 and C$^{1'}$ in **5b**) and for C$^{2'}$ in both **2b** and **5b**. These observations are also consistent with the presence of *cis* and *trans* isomers.

Table 3 Selected spectroscopic and electrochemical properties of [MoO(dithiolene)$_2$]$^{2-}$ complexes

Complex	ν(Mo=O)[a]/cm^{-1}	ν(C=C)[a]/cm^{-1}	^{1}H$_{\text{dithiolene}}$/ppm[b]	$E_{\frac{1}{2}}$[c]/mV
1	879	1516	7.13[d]	−480
2	902	1503	7.96[e]	−422
3	882	1515	7.26	−385
4	900	1503	7.59[e]	−348
5	905	1499	8.50	−280
6	886	1510	7.91	−345
7	890		8.07	−330

[a] KBr disc, as [Ph$_4$P]$^+$ salt, ν(C=C) band obscured for **7**. [b] 300 MHz ^{1}H NMR spectra unless stated otherwise, chemical shifts downfield from SiMe$_4$, value quoted is average position of two singlets, as [Bu$^n{}_4$P]$^+$ salt. [c] In dmf with [Bu$^n{}_4$N][BF$_4$] as suporting electrolyte, scan rate = 100 mV s^{-1}, peak potentials *vs.* SCE, as [Ph$_4$P]$^+$ salt. [d] At 500 MHz. [e] At 400 MHz.

IR Spectroscopy

Complexes **1**–**7** exhibit stretching frequencies in the region 879–905 cm^{-1} for ν(Mo=O) and 1499–1516 cm^{-1} for ν(C=C), these are listed in Table 3. The range of ν(Mo=O) stretching frequencies for **1**–**7** is typical for complexes containing a Mo^{IV}OS_4 unit within a square-based pyramidal geometry {*cf.* ν(Mo=O) 928 and 905 cm^{-1} in [MoO(mnt)$_2$]$^{2-}$ [36] and [MoO(bdt)$_2$]$^{2-}$,[33] respectively}. The ν(C=C) and ν(Mo=O) values are correlated; as ν(C=C) decreases ν(Mo=O) increases (see below).

Electrochemistry

All of the cyclic voltammograms recorded for these complexes in dmf featured two electroactive processes: a reversible (or quasi-reversible) oxidation process at a negative potential (*vs.* SCE) assigned to the [MoO(dithiolene)$_2$]$^-$–[MoO(dithiolene)$_2$]$^{2-}$ couple and an irreversible process in the range 365 to 500 mV assigned to the [MoO(dithiolene)$_2$]–[MoO(dithiolene)$_2$]$^-$ couple. For **5**, a second, unassigned irreversible process was observed at −635 mV. The $E_{\frac{1}{2}}$ values for the Mo^V–Mo^{IV} couples are given in Table 3; in the scan rate range 50–200 mV s^{-1}, $i_p{}^c/i_p{}^a$ was 1.0 and i_p varied linearly with the square root of the scan rate. The $E_{\frac{1}{2}}$ value of the Mo^V–Mo^{IV} couple depends upon the nature of R (see below). Differences in $E_{\frac{1}{2}}$ values for *cis* and *trans* isomers were not observed, however, the broad nature of the oxidation and reduction waves may be a consequence of the presence of the two isomers in solution.

UV/VIS spectroscopy

The susceptibility of the complexes to oxidation, especially in solution during preparation, was indicated by the ^{1}H NMR spectra (see above). In order to distinguish clearly the UV/VIS bands associated with both the [MoO(dithiolene)$_2$]$^{2-}$ and the [MoO(dithiolene)$_2$]$^-$ complexes, some of which are weak and overlap with bands of the other species, coupled spectroelectrochemical studies were performed using an OTTLE cell.[23] The information obtained is summarised in Table 4 and, as an example, the OTTLE results for **7** are presented in Fig. 6.

EPR spectroscopy

The EPR spectra at X-band were recorded as fluid and frozen

Table 4 OTTLE characteristics of the [MoO(dithiolene)$_2$]$^-$–[MoO(dithiolene)$_2$]$^{2-}$ couple

Complex	$E_{\frac{1}{2}}$[a] (Mo^V–Mo^{IV})/mV	Initial potential[b]/mV	Final potential/mV	[MoO(dithiolene)$_2$]$^{2-}$ λ/nm (ε/dm^3 mol^{-1} cm^{-1})	[MoO(dithiolene)$_2$]$^-$ λ/nm (ε/dm^3 mol^{-1} cm^{-1})	Isosbestic points/nm
1a	−480	−500	−350	556 (1092), 400 (8278)	842 (2276), 548 (1334), 380 (8079)	476
2a	−422	−460	−300	554 (359), 388 (1167), 338 (1282), 292 (1705), 276 (2450)	828 (403), 554 (368), 340 (1228), 276 (1794)	347, 516
3a	−385	−400	−340	536 (3853), 415 (12 100), 336 (14 350)	828 (3100), 531 (2710), 413 (9270), 337 (14 275)	514, 368
4a	−348	−420	−220	557 (1045), 500 (1230), 392 (6840), 337 (5221)	816 (1640), 560 (1180), 384 (3960), 339 (5230), 309 (6000)	514, 368
5a[c]	−280	−380	−150	498 (24 000), 474 (26 497), 337 (63715)	826 (5265), 470 (2660), 402 (34 940), 323 (51 874), 309 (55 619)	
7	−330	−500	−100	509 (11 207), 387 (26 284), 348 (29 353), 277 (23 599)	835 (7571), 446 (15 232), 345 (32 496), 277 (22 779)	716, 480, 427, 366, 311

[a] In dmf with [NBu$^n{}_4$][BF$_4$] as supporting electrolyte, scan rate = 100 mV s^{-1}, peak potentials *vs.* SCE, as [PPh$_4$]$^+$ salt. [b] Increased in 20 mV increments to the final potential. [c] UV/VIS spectra gradually changed with increasing applied potential up to −270 mV giving isosbestic points at 394 and 496 nm. From −270 to −150 mV, new isosbestic points at 721, 461 and 381 nm were observed. On completion of the oxidation experiment, the initial spectrum was obtained on application of the initial potential.

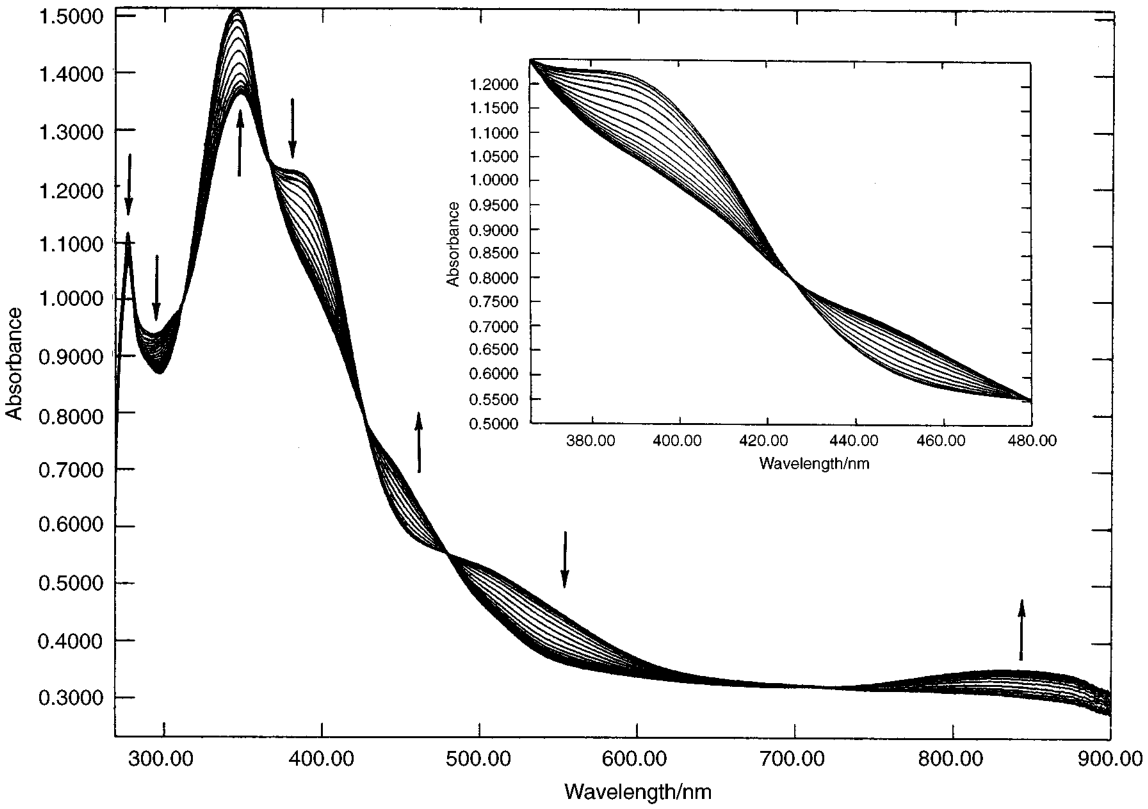

Fig. 6 The UV/VIS spectra, using an OTTLE cell, of $[MoO\{NC(H)N(Me)_2\text{-ptedt}\}_2]^-$–$[MoO\{NC(H)N(Me)_2\text{-ptedt}\}_2]^{2-}$ in dmf *vs.* SCE with $[NBu^n_4][BF_4]$ as supporting electrolyte and a Pt–Rh gauze working electrode and an expansion of the region 360–480 nm (inset). Arrows indicate the transition from Mo^{IV} to Mo^V

solutions in dmf for compounds **1**–**6** oxidised with $[FeCp_2][PF_6]$. The EPR spectrum of a solution of each of the $[MoO(\text{dithiolene})_2]^{2-}$ complexes, in which the ^1H NMR had been broadened by (presumably) aerial oxidation and the corresponding system oxidised with $[FeCp_2][PF_6]$ were identical. Apart from some slight differences in the linewidth, all of the EPR spectra of the Mo^V species reported herein were essentially superimposable within each phase of measurement. Therefore, the EPR parameters are characteristic of $[MoO(\text{dithiolene})_2]^-$ [where dithiolene = $^-SC(R){=}C(H)S^-$], in this geometry. The values of g_{iso} and A_{iso} of 1.995 and 27.0×10^{-4} cm^{-1} are consistent with the parameters for $[MoO(mnt)_2]^-$ (1.991 and 28.3×10^{-4} cm^{-1})[36] and $[MoO(SCH_2CH_2S)_2]^-$ (1.999, 30.3×10^{-4} cm^{-1}),[37] which indicate predominantly metal-based character for the unpaired electron. In frozen solution the g values are rhombic (g_1 2.021, g_2 1.987, g_3 1.976). Assuming a coincidence of the g and A matrices, measurement of the anisotropic spectrum and the subsequent simulation yields values for the rhombic metal hyperfine interaction; A_1 43.0×10^{-4}, A_2 16.8×10^{-4} and A_3 34.6×10^{-4} cm^{-1}. A comparison of experimental and simulated spectra for **4** is given in Fig. 7. The average anisotropic parameters, g_{av} (1.995) and A_{av} (31.5×10^{-4} cm^{-1}) were in reasonable agreement with the measured isotropic values, g_{iso} and A_{iso}, and this confirms that there has been no marked perturbation of the complex upon freezing.

Discussion

The $[MoO(\text{dithiolene})_2]^{2-}$ complexes display a range of spectroscopic and redox properties which serve to characterise these species. The physical properties vary in a manner consistent with the electronic influences of the different R groups operating in an $[MoO(\text{dithiolene})_2]^{n-}$ (n = 1 or 2) framework of essentially constant geometry.

The aromatic character of the dithiolene proton is attributed to the presence of the metallocycle and is evidenced by the ^1H NMR resonances in the range δ 7.0–8.5. The relative chemical shifts of the dithiolene ^1H NMR resonances for complexes **1**–**7** is: **5** > **7** ≈ **2** ≈ **6** > **4** > **3** > **1**. This trend can be rationalised by a consideration of both inductive effects and the relative ability of the R group to stabilise a resonance form in which positive charge is localised at the C atom carrying the dithiolene proton (Scheme 3). Hence when R = phenyl, no such resonance forms

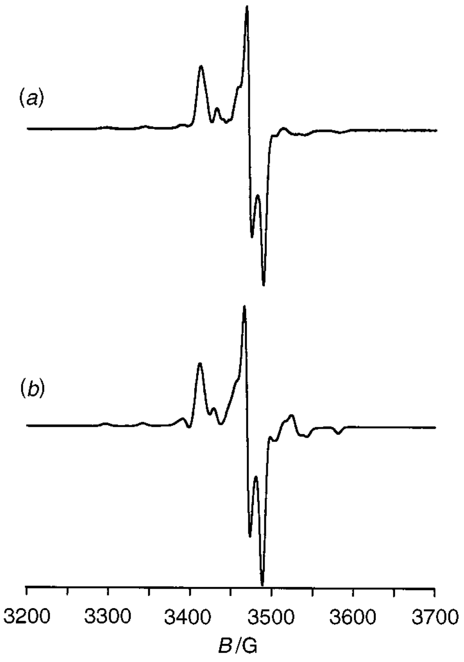

Fig. 7 (*a*) Experimental X-band EPR spectrum of $[MoO(4\text{-pedt})_2]^-$ in dmf solution at 150 K, and (*b*) simulation with the spin-Hamiltonian parameters $g_1 = 2.021$, $g_2 = 1.987$, $g_3 = 1.976$, $A_1 = 43.0 \times 10^{-4}$ cm^{-1}, $A_2 = 16.8 \times 10^{-4}$ cm^{-1}, $A_3 = 34.6 \times 10^{-4}$ cm^{-1} with Gaussian linewidths of W_1 = 10 G, W_2 = 6 G and W_3 = 7 G

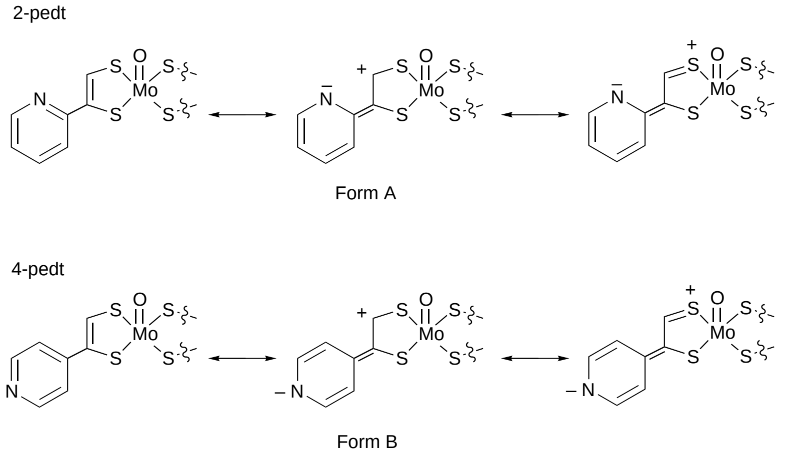

Scheme 3

can be written, with the result that the chemical shift of the dithiolene proton in **1** is the most shielded of the series. Similarly, no such resonance form can be written when the ligand is 3-pedt, hence the difference in dithiolene proton resonances in **1** and **3** is a measure of the relative inductive effects of the aromatic groups. In contrast, forms A and B (Scheme 3), indicating a mesomeric drift of electron density to the nitrogen atom, can be written for **2** and **4**, respectively. Resonance forms analogous to those for **2** may be written for **5**, **6** and **7**. This results in a greater resonance effect and a resultant deshielding of the dithiolene proton chemical shift with respect to that in **3**. The downfield shift of *ca.* 0.35 ppm between the chemical shifts of the dithiolene protons of **2** and **4** can be attributed to the proximity of nitrogen atom to the dithiolene proton. On this basis, the quinoxaline ring in **5** must exert a larger electron withdrawing effect than both the phenyl in **1** and the pyridines in **2**, **3** and **4**, for the largest deshielding effect is observed for the dithiolene ^{1}H NMR resonance in **5**. The pterin ligands in **6** and **7** lead to chemical shifts for the dithiolene protons similar to those for compound **2** containing the 2-pedt ligand.

The chemical shifts for the C-atom carrying the dithiolene proton in the ^{13}C NMR spectra of **1**, **2** and **5** followed the same trend as was observed for the dithiolene protons in the ^{1}H NMR spectra (see above).

The discussion of inductive effects and resonance forms presented above for the dithiolene ^{1}H NMR chemical shifts appears to be relevant to the observed trends in ν(C=C) and ν(Mo=O) stretching frequencies. Thus, the ν(C=C) stretching frequency varies from 1499 cm^{-1} in **5** to 1516 cm^{-1} in **1**, as: **5** < **2** ≈ **4** < **6** < **3** ≈ **1** (Table 3) [the ν(C=C) for **7** could not be assigned due to overlapping bands]. The reverse order applies for ν(Mo=O) with values ranging from 905 cm^{-1} in **5** to 879 cm^{-1} in **1**. Thus, as the electronic structure (Scheme 3) favours more contribution from an (S)C–C(S) bond, lowering the ν(C=C) stretching frequency, this leads to more electronic charge being drawn from S; the latter will contribute less to the pπ–Mo dπ (d_{xz}, d_{yz}) bonding and hence allow more O pπ–Mo dπ bonding resulting in an increase in the ν(Mo=O) stretching frequency. Interestingly, when the dithiolene protons in **1a** were exchanged for deuterium atoms, in **1c**, no change was observed for the ν(Mo=O) frequency (879 cm^{-1}), as might be expected, however the ν(C=C) frequency was shifted from 1516 to 1510 cm^{-1} due to isotopic substitution. The observation of a band attributed to a ν(C=C) stretching frequency at 1568 cm^{-1} in the resonance-Raman spectrum of the reduced (Mo^{IV}) form of DMSOR from *Rhodobacter sphaeroides*[38] has been advanced as supporting evidence for the presence of an ene–1,2-dithiolate group as a ligand of Mo in these enzymes. Hence, the values for the ν(C=C) stretching frequencies reported herein will be useful as calibrants for the ν(C=C) stretching frequencies of oxomolybdenum enzymes. Further studies, including resonance-Raman investigations of our systems and normal coordinate analyses, are planned to improve the understanding of this situation.

The general trend in the $E_{\frac{1}{2}}$ values can be addressed on the basis of the relative inductive nature of the R group as argued above. As the ability of R to stabilise the resonance forms A or B in Scheme 3 increases (*i.e.* the relative electron withdrawing nature of the R group increases), the $E_{\frac{1}{2}}$ values for the Mo^{V}–Mo^{IV} couple would be expected to be less negative (or more positive), *i.e.* the complex should be more difficult to oxidise. This expectation is realised in the overall sense that for **1** and **5**, containing the least and most electron withdrawing ligands, respectively, the corresponding $E_{\frac{1}{2}}$ values for the Mo^{V}–Mo^{IV} couple are −480 and −280 mV *versus* SCE, respectively and that the $E_{\frac{1}{2}}$ values for the Mo^{V}–Mo^{IV} couples in the pedt complexes **2**, **3**, **4** and the pterins **6** and **7** lie between these limits. The trend within the pedt series follows the proximity of the pyridinyl nitrogen atom to the metal centre, hence $E_{\frac{1}{2}}$ values for the Mo^{V}–Mo^{IV} couples in the pedt complexes fall in the order: **2** > **3** > **4**. The overall trend is **5** < **7** < **6** < **4** < **3** < **2** < **1**. The irreversibility of the putative Mo^{VI}–Mo^{V} couple is not unexpected since no [Mo^{VI}O(dithiolene)$_2$] complexes have been isolated; the overall oxidation of a MoO^{2+} centre to Mo^{VI} generally involves the addition of an oxo group.[39,40]

The relatively low and negative potential, *vs.* SCE, of the reversible, one-electron Mo^{V}–Mo^{IV} couple which varies with R, required the use of the OTTLE technique to generate each oxidation state discretely in solution for UV–VIS spectroscopic studies. These spectra were consistent with the presence of the MoOS_4 chromophore in both Mo^{V} and Mo^{IV} states and were essentially invariant with respect to the nature of aromatic substituent of the dithiolene. The observation of isosbestic points in each of the OTTLE spectra indicates that the oxidation of Mo^{IV} to Mo^{V} in these complexes progresses smoothly, with no intermediates or large structural change. This might be anticipated from the geometries of [MoO(dithiolene)$_2$]$^{2-/-}$ which show little structural variance.[33] Compound **5** exhibited an atypical result. The lowest energy band of each of the Mo^{V} species was assigned to a d–d transition ($b_2 \longrightarrow e$) by analogy with [MoOCl$_4$]$^-$;[41–43] the larger extinction coefficients in the MoOS_4 complexes arising from intensity stealing or charge transfer ($S \longrightarrow Mo$) at the same energies. Assignment of higher energy bands requires magnetic circular dichroism (MCD) studies analogous to those for DMSOR.[44,45] However, the lack of correlation in the UV/VIS data reported herein and those for DMSOR illustrates the difference in electronic structure, as a possible consequence of the unique co-ordination at Mo in the enzyme, between the two systems.

The invariance of the EPR spectra within the series of compounds synthesised herein is in contrast to the trends observed in NMR and IR spectroscopy and electrochemical studies.

However, the occurrence of essentially the same spectra for the entire series of compounds **1** to **6** is consistent with a common structural type, the square-based pyramidal geometry, being present throughout the series of complexes. Furthermore, the essential invariance of the EPR spectra is consistent with the unpaired electron of the Mo^V centre occupying the b_2 orbital of a C_{4v} $MoOS_4$ moiety, orthogonal to both the S σ and π orbitals through which the resonance and inductive effects of the R group influence the properties of the Mo centre. Thus, the EPR properties serve to characterise a $[MoO(dithiolene)_2]^-$ centre, where the dithiolene is asymmetric, and in this context we note the difference between these parameters and those reported for DMSOR,[46,47] which highlights the effect of the special co-ordination geometry of the Mo in this enzyme.

Conclusion

The recent publications[11–13] documenting the structure of the active (metal) site of the oxotransfer molybdoenzymes have identified the co-ordination of molybdenum by an asymmetric dithiolene (ene–1,2-dithiolate) ligand carried on the side chain of a reduced pterin. We have developed a general route to deliver an asymmetric dithiolene, protected either as a 1,3-dithiol-2-one or a 2-(*N*,*N*-dimethylimino)-1,3-dithiolium hydrogensulfate salt, to an oxomolybdenum(IV) centre. The asymmetric dithiolene is released by controlled base hydrolysis in hydroxylic media and the extent of complexation, to preclude formation of a tris(dithiolene) complex, is directed by the use of *trans*-$[MoO_2(CN)_4]^{4-}$ as the starting material. The route has allowed a range of aromatic heterocyclic substituents (pyridines, quinoxaline and pterin) to be bound in the $^-SC(H)=C(R)S^-$ moiety.

The bis(dithiolene)oxomolybdate(IV) complexes display a range of spectroscopic and redox properties which characterise these species and vary in a manner consistent with the nature of the R group. Thus, the aromatic character of the dithiolene proton, derived from the presence of the metallocycle, is evidenced by chemical shifts in the range δ 7.0–8.5. The relatively low and negative potential, *versus* SCE, of the reversible, one-electron Mo^V–Mo^{IV} couple which varies with R, required the use of the OTTLE technique to generate either oxidation state discretely in solution for UV/VIS spectroscopic studies. These spectra were consistent with the presence of the $MoOS_4$ chromophore in these states, were essentially invariant with respect to the aromatic substituent of the dithiolene and showed that the redox event is a simple process as judged by the appearance of isosbestic points in the spectra. Similarly, the EPR parameters of the complexes in the Mo^V state are essentially invariant with respect to substituent.

The prototypical structure in this series of complexes is afforded by the crystallographic characterisation of $[PPh_4]_2[MoO(sdt)_2]\cdot EtOH$, which shows the expected square-based pyramidal geometry at Mo and the range of spectroscopic and electrochemical studies accomplished show that this basic geometry is retained in both the solid state and in solution throughout this series of complexes. The occurrence of *cis* and *trans* isomers within the series, as evidenced by ^1H and ^{13}C NMR studies, is expected for the asymmetric dithiolenes and should be viewed in the context of the cisoid nature of the geometry of the molybdopterins in the studies of native (oxidised) DMSOR (*R. capsulatus* and *R. sphaeroides*)[11–13] and aldehyde ferredoxin oxidoreductase (*Pyrococcus furiosus*).[16] Our studies demonstrate that there is no apparent difference between the electronic properties of the metal in these two isomers and also that the pterin substituent does not produce any marked variation in either the spectroscopic or electrochemical properties beyond what may have been reasonably extrapolated from the other aromatic heterocycles.

Although spectroscopic and electrochemical characterisation of the $[MoO(dithiolene)_2]^{-/2-}$ complexes demonstrate a variance from those properties of the oxotransfer molybdoenzymes which they model, this series of compounds, especially those containing the pterin moiety, represent the closest structural models available to date.

Acknowledgements

We thank the BBSRC for post-doctoral (E. S. D.) and the EPSRC for post-doctoral (A. Dinsmore) and student (A. D. and C. R. W.) support of this work. Drs. F. E. Mabbs and E. J. L. McInnes of the EPSRC c.w. EPR service for spectra and analysis. Dr. S. Bailey for crystallographic data. We also thank Drs. M. W. Whiteley and M. Helliwell for helpful discussions.

References

1 J. A. Pateman, D. J. Cove, B. M. Rever and D. B. Roberts, *Nature* (*London*), 1964, **201**, 58.

2 P. A. Ketchum, H. Y. Cambrier, W. A. Frazier, C. H. Madansky and A. Nason, *Proc. Natl. Acad. Sci. USA*, 1970, **66**, 1016; A. Nason, K. Y. Lee, S. S. Pan, P. A. Ketchum, A. Lamberti and J. Devries, *ibid.*, 1971, **68**, 3242.

3 V. K. Shah and W. J. Brill, *Proc. Natl. Acad. Sci. USA*, 1977, **74**, 3249; P. T. Pienkos, V. K. Shah and W. Brill, *ibid.*, 5468.

4 In the light of several previous reviews on Moco and related topics [refs. 5, 6(*a*) and S. Goswami, *Heterocycles*, 1993, **35**, 1551] we reference here only key original papers concerned with the development of the subject.

5 J. L. Johnson, in *Molybdenum and Molybdenum Containing Enzymes*, ed. M. P. Coughlan, Pergamon Press, Oxford, 1980, pp. 345–383; J. C. Wootton, R. E. Nicolson, J. M. Cock, D. E. Walters, J. F. Burke, W. A. Doyle and R. C. Bray, *Biochim. Biophys. Acta*, 1991, **1057**, 157.

6 (*a*) J. L. Johnson, in *The Metabolic Basis of Inherited Disease*, eds. C. R. Scriver, A. L. Beaudet, W. S. Sly and D. Valle, McGraw Hill, New York, 1989, p. 1463; (*b*) G. K. Brown, R. D. Scholeum, H. B. Croll, J. E. Wraith and J. J. McGill, *Neurology*, 1989, **39**, 252.

7 *Molybdenum Enzymes*, ed. T. G. Spiro, John Wiley and Sons, New York, 1985; *Molybdenum Enzymes, Cofactors and Model Systems*, eds. E. I. Stiefel, D. Coucouvanis and W. E. Newton, *ACS Symposium Series 535*, 1993; J. H. Enemark and C. S. Young, *Adv. Inorg. Chem.*, 1994, **40**, 1; D. Collison, C. D. Garner and J. A. Joule, *Chem. Soc. Rev.*, 1996, **25**, 25; R. Hille, *Chem. Rev.*, 1996, **96**, 2757.

8 J. L. Johnson, B. E. Hainline and K. V. Rajagopalan, *J. Biol. Chem.*, 1980, **255**, 1783; J. L. Johnson, B. E. Hainline, K. V. Rajagopalan and B. H. Arison, *J. Biol. Chem.*, 1984, **259**, 5414.

9 E. C. Taylor, P. S. Ray, I. S. Darwish, J. L. Johnson and K. V. Rajagopalan, *J. Am. Chem. Soc.*, 1989, **111**, 7664.

10 M. J. Romão, M. Archer, I. Moura, J. J. G. Moura, J. LeGall, R. Engh, M. Schneider, P. Hof and R. Huber, *Science*, 1995, **270**, 1170.

11 H. Schindelin, C. Kisker, J. Hilton, K. V. Rajagopalan and D. C. Rees, *Science*, 1996, **272**, 1615.

12 F. Schneider, J. Löwe, R. Huber, H. Schindelin, C. Kisker and J. Knäblein, *J. Mol. Biol.*, 1996, **263**, 53.

13 S. Bailey, A. S. McAlpine, E. M. H. Duke, N. Benson and A. G. McEwan, *Acta Crystallogr., Sect. D*, 1996, **52**, 194; S. Bailey, A. S. McAlpine, A. G. McEwan and A. L. Shaw, unpublished work.

14 J. C. Boyington, V. N. Gladyshev, S. V. Khangulov, T. C. Stadtman and P. D. Sun, *Science*, 1997, **275**, 1305.

15 M. K. Chan, S. Mukund, A. Kletzin, M. W. W. Adams and D. C. Rees, *Science*, 1995, **267**, 1463.

16 J. Van de Poel and H. M. Neumann, *Inorg. Chem.*, 1968, **7**, 2086.

17 S. J. Lippard and B. J. Russ, *Inorg. Chem.*, 1967, **6**, 1943.

18 D. J. Rowe, C. D. Garner and J. A. Joule, *J. Chem. Soc., Perkin Trans. 1*, 1985, 1907.

19 A. Dinsmore, J. H. Birks, C. D. Garner and J. A. Joule, *J. Chem. Soc., Perkin Trans. 1*, 1997, 801.

20 A. K. Bhattacharya and A. G. Hortmann, *J. Org. Chem.*, 1974, **39**, 95.

21 C. J. Pickett, *J. Chem. Soc., Chem. Commun.*, 1985, 323.

22 R. R. Gagné, C. A. Koval and G. C. Lisensky, *Inorg. Chem.*, 1980, **19**, 2854.

23 R. M. Murray, W. R. Heineman and G. W. O'Dom, *Anal. Chem.*, 1967, **39**, 1666.

24 N. Walker and D. Stuart, *Acta Crystallogr., Sect. A*, 1983, **39**, 158.

25 G. M. Sheldrick, C. Krueger and R. Goddard, *Crystallographic Computing 3*, Oxford University Press, 1985, p. 175.

26 D. T. Cromer and J. T. Waber, *International Tables for X-Ray Crystallography*, Kynoch Press, Birmingham, 1974, vol. 4, Table 2.2A.
27 D. T. Cromer and J. T. Waber, *International Tables for X-Ray Crystallography*, Kynoch Press, Birmingham, 1974, vol. 4, Table 2.3.1.
28 TEXSAN-TEXRAY Structure Analysis Package, Molecular Structure Corporation, Houston, TX, 1985.
29 A. L. Spek, *Acta Crystallogr., Sect. A*, 1990, **46**, C34.
30 J. A. McCleverty, *Prog. Inorg. Chem.*, 1969, **10**, 49.
31 S. Boyde, C. D. Garner, J. A. Joule and D. J. Rowe, *J. Chem. Soc., Chem. Commun.*, 1987, 800.
32 S. Motherwell and W. Clegg, PLUTO Program for Plotting Molecular and Crystal Structures, University of Cambridge, 1978.
33 S. Boyde, S. R. Ellis, C. D. Garner and W. Clegg, *J. Chem. Soc., Chem. Commun.*, 1986, 1541.
34 B. Götz, F. Knoch and H. Kisch, *Chem. Ber.*, 1996, **129**, 33.
35 J. K. Hsu, C. J. Bonangelino, S. P. Kaiwar, C. M. Boggs, J. C. Fettinger and R. S. Pilato, *Inorg. Chem.*, 1996, **35**, 4743.
36 S. K. Das, P. K. Chaudhury, D. Biswas and S. Sarker, *J. Am. Chem. Soc.*, 1994, **116**, 9061.
37 S. R. Ellis, D. Collison, C. D. Garner and W. Clegg, *J. Chem. Soc., Chem. Commun.*, 1986, 1483.
38 S. Gruber, L. Kilpatrick, N. R. Bastian, K. V. Rajagopalan and T. G. Spiro, *J. Am. Chem. Soc.*, 1990, **112**, 8179.
39 H. Oku, N. Ueyama, M. Kondo and A. Nakamura, *Inorg. Chem.*, 1994, **33**, 209.
40 N. Ueyama, H. Oku, M. Kondo, T. Okamura, N. Yoshinaga and A. Nakamura, *Inorg. Chem.*, 1996, **35**, 643.
41 E. A. Allen, B. J. Brisdon, D. A. Edwards, G. W. A. Fowles and R. G. Williams, *J. Chem. Soc.*, 1963, 4649.
42 F. E. Mabbs, I. H. Hillier, J. Kendrick and C. D. Garner, *Nature* (*London*), 1975, **258**, 138.
43 C. D. Garner, L. Hill, N. C. Howlander, M. R. Hyde, F. E. Mabbs and V. I. Routledge, *J. Less Common Met.*, 1977, **54**, 27.
44 M. G. Finnegan, J. Hilton, K. V. Rajagopalan and M. K. Johnson, *Inorg. Chem.*, 1993, **32**, 2616.
45 N. Benson, J. A. Farrar, A. G. McEwan and A. J. Thomson, *FEBS Lett.*, 1992, **307**, 169.
46 B. Bennett, N. Benson, A. G. McEwan and R. C. Bray, *Eur. J. Biochem.*, 1994, **225**, 321.
47 G. N. George, J. Hilton and K. V. Rajagopalan, *J. Am. Chem. Soc.*, 1996, **118**, 1113.

Received 28*th May* 1997; *Paper* 7/03682E